






Article

Coumarin Derivatives Exert Anti-Lung Cancer Activity by Inhibition of Epithelial–Mesenchymal Transition and Migration in A549 Cells

Rodrigo Santos Aquino de Araújo ^{1,2}, Julianderson de Oliveira dos Santos Carmo ³, Simone Lara de Omena Silva ³, Camila Radelley Azevedo Costa da Silva ³, Tayhana Priscila Medeiros Souza ³, Natália Barbosa de Mélo ¹, Jean-Jacques Bourguignon ², Martine Schmitt ², Thiago Mendonça de Aquino ⁴, Renato Santos Rodarte ³, Ricardo Olímpio de Moura ¹, José Maria Barbosa Filho ⁵, Emiliano Barreto ^{3,*} and Francisco Jaime Bezerra Mendonça-Junior ^{1,5,*}

- ¹ Laboratory of Synthesis and Drug Delivery, Department of Biological Sciences, State University of Paraíba, João Pessoa 58429-500, PB, Brazil; rodrigobiologojp@gmail.com (R.S.A.d.A.); nataliamelo926@gmail.com (N.B.d.M.); ricardo.olimpiodemoura@gmail.com (R.O.d.M.)
- ² Laboratoire d'Innovation Thérapeutique, UMR 7200, Labex Medalis, CNRS, Université de Strasbourg, Faculté de Pharmacie, 74 route du Rhin, BP 60024, 67401 Illkirch, France; jbbourguignon@unistra.fr (J.-J.B.); mschmitt@unistra.fr (M.S.)
- ³ Institute of Biological and Health Sciences, Federal University of Alagoas, Maceio 57072-900, AL, Brazil; julianderson.oliveira.bio@gmail.com (J.d.O.d.S.C.); omena.simone@hotmail.com (S.L.d.O.S.); camilaradelley@gmail.com (C.R.A.C.d.S.); medeiros.tayhana@gmail.com (T.P.M.S.); rrodarte@icbs.ufal.br (R.S.R.)
- ⁴ Research Group on Therapeutic Strategies—GPET, Institute of Chemistry and Biotechnology, Federal University of Alagoas, Maceio 57072-900, AL, Brazil; thiago.aquino@iqb.ufal.br
- ⁵ Post-Graduate Program in Natural and Synthetic Bioactive Products, Federal University of Paraíba, João Pessoa 58051-900, PB, Brazil; barbosa.ufpb@gmail.com
- * Correspondence: emilianobarreto@icbs.ufal.br (E.B.); franciscojbmendonca@yahoo.com.br (F.J.B.M.-J.)
- † These authors contributed equally to this work.



Citation: de Araújo, R.S.A.; Carmo, J.d.O.d.S.; de Omena Silva, S.L.; Costa da Silva, C.R.A.; Souza, T.P.M.; Mélo, N.B.d.; Bourguignon, J.-J.; Schmitt, M.; Aquino, T.M.d.; Rodarte, R.S.; et al. Coumarin Derivatives Exert Anti-Lung Cancer Activity by Inhibition of Epithelial–Mesenchymal Transition and Migration in A549 Cells. *Pharmaceuticals* **2022**, *15*, 104. <https://doi.org/10.3390/ph15010104>

Academic Editors: Urszula K. Komarnicka, Monika Lesiów and Sabina Jaros

Received: 20 November 2021

Accepted: 6 January 2022

Published: 17 January 2022

Publisher's Note: MDPI stays neutral with regard to jurisdictional claims in published maps and institutional affiliations.



Copyright: © 2022 by the authors. Licensee MDPI, Basel, Switzerland. This article is an open access article distributed under the terms and conditions of the Creative Commons Attribution (CC BY) license (<https://creativecommons.org/licenses/by/4.0/>).

Abstract: A series of coumarin derivatives and isosteres were synthesized from the reaction of triflic intermediates with phenylboronic acids, terminal alkynes, and organozinc compounds through *palladium*-catalyzed cross-coupling reactions. The *in vitro* cytotoxic effect of the compounds was evaluated against two non-small cell lung carcinoma (NSCLC) cell lines (A-549 and H2170) and a normal cell line (NIH-3T3) using cisplatin as a reference drug. Additionally, the effects of the most promising coumarin derivative (**9f**) in reversing the epithelial-to-mesenchymal transition (EMT) in IL-1 β -stimulated A549 cells and in inhibiting the EMT-associated migratory ability in A549 cells were also evaluated. **9f** had the greatest cytotoxic effect ($CC_{50} = 7.1 \pm 0.8$ and 3.3 ± 0.5 μ M, respectively against A549 and H2170 cells) and CC_{50} value of 25.8 μ M for NIH-3T3 cells. **9f** inhibited the IL-1 β -induced EMT in epithelial cells by inhibiting the F-actin reorganization, attenuating changes in the actin cytoskeleton reorganization, and downregulating vimentin in A549 cells stimulated by IL-1 β . Treatment of A549 cells with **9f** at 7 μ M for 24 h significantly reduced the migration of IL-1 β -stimulated cells, which is a phenomenon confirmed by qualitative assessment of the wound closure. Taken together, our findings suggest that coumarin derivatives, especially compound **9f**, may become a promising candidate for lung cancer therapy, especially in lung cancer promoted by NSCLC cell lines.

Keywords: anticancer activity; lung cancer; non-small-cell lung cancer; epithelial–mesenchymal transition; metastasis; coumarin derivative

1. Introduction

Cancer is characterized by cells with uncontrolled division, genome heterogeneity, and invasiveness to other tissues via blood or lymph nodes. According to the World Health

Organization (WHO) reports, almost nine million cancer-related deaths annually occur [1]. Among cancers, lung cancer is one of the most common types, with a mortality rate of around 18.4% according to the GLOBOCAN report [2].

Cancer metastasis is defined as the formation of new tumors in tissues away from the primary site; it accounts for a vast majority of the morbidity and mortality of patients and is associated with about 90% of all cancer-associated deaths [3,4]. In the past decade, an increasing number of studies have provided strong evidence to proposed that epithelial–mesenchymal transition (EMT)—a known cellular program allowing polarized cells to shift to a mesenchymal phenotype with increased cellular motility [5]—has a central role in cancer progression and metastatic dissemination [6–8]. For this reason, the EMT has become as a target of interest for anticancer therapy [9,10].

Furthermore, cancer therapy is complex due mainly to drug resistance, which leads to less effectiveness of the anticancer agents. Therefore, the discovery and development of new chemotherapeutic agents with greater efficacy is a very urgent need.

Coumarins are a class of secondary metabolites chemically characterized by the fusion of a benzene with an α -pirone ring [11]. Their pharmacological applications are widely described [12–17], highlighting its applications in the treatment of several human cancer and in the inhibition of cell growth of several cancer cell lines [18–27], including lung cancer [21,28–37]. Its low toxicities [38,39], associated with its potential to inhibit several proteins associated with lung cancer (tyrosine kinase, telomerase, NF- κ B, ERK1/2, EGFR, STAT proteins, HSP 90, PI3K, Bax, among others) [24,26,28], makes them promising prototypes for the development of new anti-lung cancer drugs.

In view of the above, the aim of this study was to synthesize a series of coumarins derivatives obtained through palladium-catalyzed cross-coupling reactions (PCCCR) and evaluate their cytotoxic effects *in vitro* in two non-small two cell lung carcinoma (NSCLC) cell lines (A549 and H2170). Additionally, we investigated the potential of the most promising coumarin derivative (**9f**) in reversing the epithelial-to-mesenchymal transition (EMT) in IL-1 β -stimulated A549 cells, and in inhibiting the EMT-associated migratory ability in A549 cells.

2. Results and Discussion

2.1. Chemistry

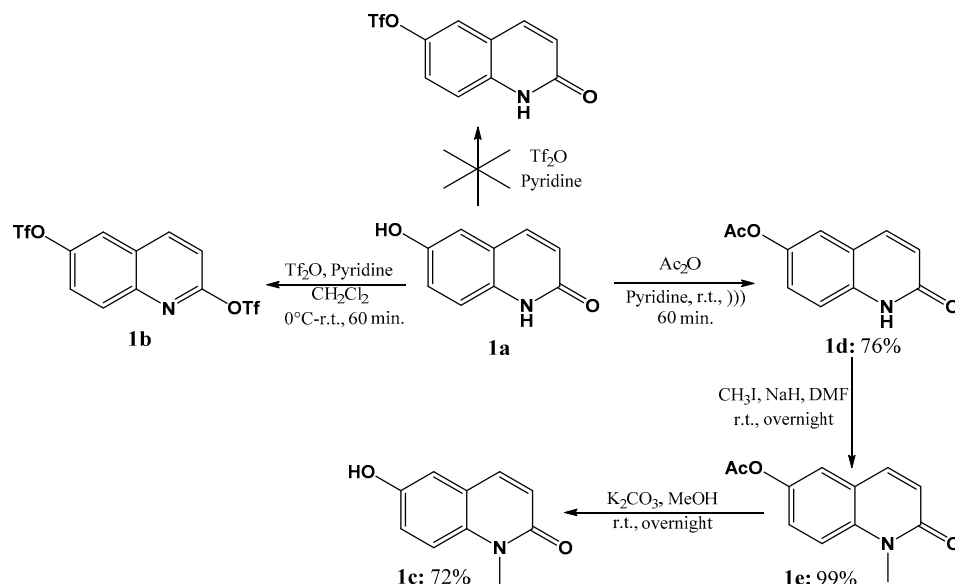
The synthesis of the coumarin core can be performed by different synthetic methodologies, among which the most common are Pechmann, Wittig, Knoevenagel, and Perkin reactions [11]. Cross-coupling reactions catalyzed by transition metals, such as the Suzuki–Miyaura, Negishi [40], and Sonogashira [41] reactions, have become powerful alternatives to the formation of carbon–carbon bonds [42,43] and allowed the introduction of various substituents in all positions of the basic nucleus, leading to analogous, homologous, or libraries of compounds [44].

The preparation of target compounds (coumarins, quinolones, and chromen-4-ones) involved the formation of triflic methanesulfonate derivatives as key intermediates **4**, **5a–b**, and **6**, thanks to the cross-coupling reactions. 6- and 7-hydroxycoumarin **2a–b** and 6-hydroxyquinolone **1a** are commercially available, and 3-hydroxy-chromen-4-one **3** was synthesized following a reported preparation [45]. Attempts to prepare 6-OTf quinolone from **1a** and triflic anhydride resulted exclusively in the formation of the 2,6 di-triflic adduct **1b**. Therefore, our efforts focused on the preparation of N-Me quinolone **1c**. However, N-alkylation of quinolone **1a** needed a first transient protection of the phenol by an acetyl group (compounds **1d–e**) according to Scheme 1.

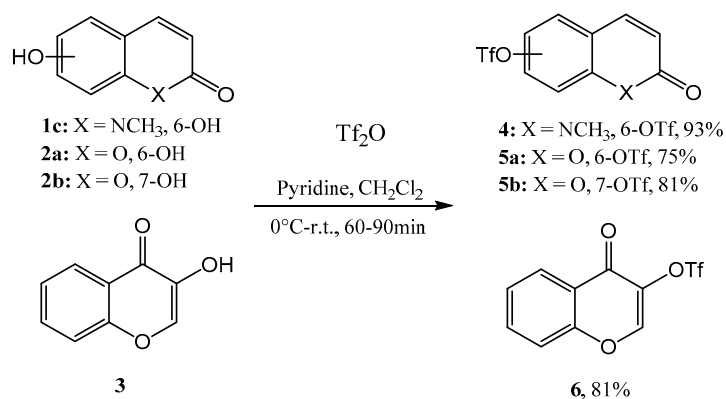
Reaction of the respective hydroxyl cores (cpds **1c**, **2a–b**, and **3**) with triflic anhydride in the presence of pyridine afforded the corresponding triflic intermediates **4**, **5a–b**, and **6** in high yields ($\geq 75\%$), as illustrated in Scheme 2.

With triflic intermediates **4**, **5a,b**, and **6** in hand, our attention next turns to the Suzuki–Miyaura cross-coupling reaction. Reaction with various boronic acids enables the preparation of a small library of 6- and 7-substituted coumarins (cpds **8a–f**, **9a–g**).

The use of a catalytic amount of tetrakis(triphenylphosphine) palladium(0) (5.0 mol %) in the presence of NaHCO₃ as a base led efficiently to the target compounds (see Table 1). However, for the introduction of a pyridine moiety in the coumarin structure, K₃PO₄ was preferred over NaHCO₃ (Table 1, cpds **8d** and **9g**). For these 2 cpds, the reaction was performed in Toluene/EtOH/H₂O and yielded the expected compounds **8d** and **9g** in 74% and 82% yields, respectively. Starting from the Otf-flavone derivative **6**, the use of Pd(OAc)₂ (5.0 mol %) in the presence of KF furnished **10** in moderate yield (50%) (Scheme 3).



Scheme 1. Synthesis of 1-methyl-6-hydroxy-quinol-2-one (**2c**).



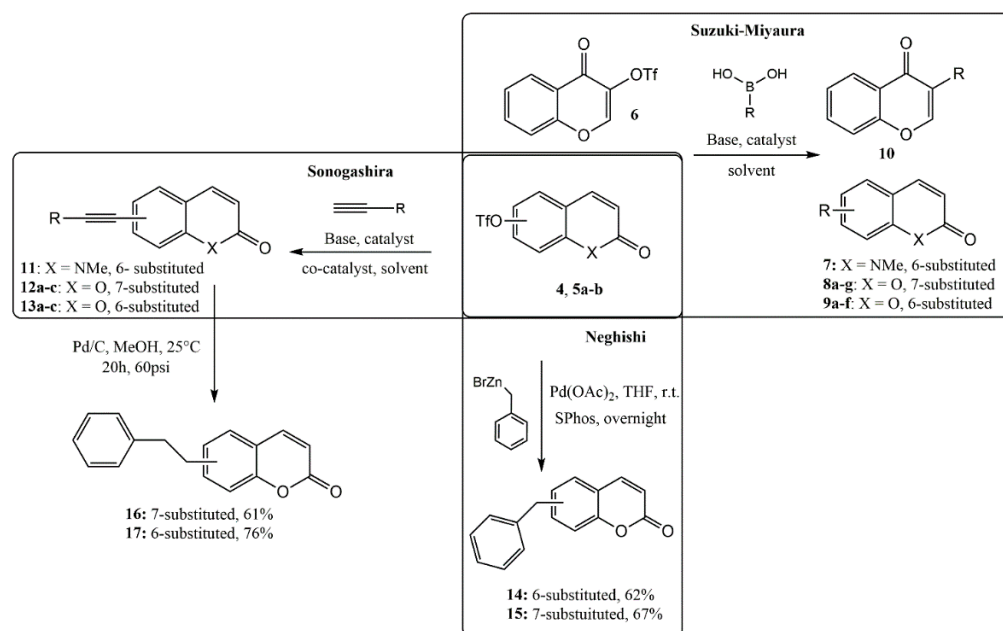
Scheme 2. Synthesis of triflic intermediates **4**, **5a–b**, **6**.

Table 1. Preparation of compounds **7**, **8a–g**, **9a–f**, and **10** through Suzuki–Miyaura conditions.

Cpd	X	R	Base	Catalyst. (5.0 mol %)	Solvent	Yield (%)
8a	O	7-(4-OCH ₃)-Ph	NaHCO ₃	Pd(PPh ₃) ₄	MeOH	71
8b	O	7-(2-OCH ₃)-Ph	NaHCO ₃	Pd(PPh ₃) ₄	MeOH	84
8c	O	7-(2-Cl)-Ph	NaHCO ₃	Pd(PPh ₃) ₄	MeOH	71
8d	O	7-(Pyridin-4-yl)	K ₃ PO ₄	Pd(PPh ₃) ₄	Toluene/EtOH/H ₂ O (4:1:1)	74
8e	O	7-(4-CF ₃)-Ph	NaHCO ₃	Pd(PPh ₃) ₄	MeOH	78
8f	O	7-(3,4-Cl)-Ph	NaHCO ₃	Pd(PPh ₃) ₄	MeOH	59
9a	O	6-(4-OCH ₃)-Ph	NaHCO ₃	Pd(PPh ₃) ₄	MeOH	73
9b	O	6-(3-OCH ₃)-Ph	NaHCO ₃	Pd(PPh ₃) ₄	MeOH	71
9c	O	6-(2-OCH ₃)-Ph	NaHCO ₃	Pd(PPh ₃) ₄	MeOH	76

Table 1. Cont.

Cpd	X	R	Base	Catalyst. (5.0 mol %)	Solvent	Yield (%)
9d	O	6-(4-Cl)-Ph	NaHCO ₃	Pd(PPh ₃) ₄	MeOH	45
9e	O	6-(2-Cl)-Ph	NaHCO ₃	Pd(PPh ₃) ₄	MeOH	71
9f	O	6-(3,4-Cl)-Ph	NaHCO ₃	Pd(PPh ₃) ₄	MeOH	68
9g	O	6-(Pyridin-4-yl)	K ₃ PO ₄	Pd(PPh ₃) ₄	Toluene/EtOH/H ₂ O (4:1:1)	82
7	NCH ₃	6-(4-OCH ₃)-Ph	NaHCO ₃	Pd(PPh ₃) ₄	MeOH	81
10	-	3-(4-Ome)-Ph	KF	Pd(Oac) ₂	MeOH	50



Scheme 3. Palladium-catalyzed cross-coupling reactions to synthesized coumarin, quinolones, and chromen-4-one derivatives.

Sonogashira reaction with different terminal alkynes resulted in seven compounds (Table 2).

Table 2. Preparation of compounds **11**, **12a–c**, and **13a–c** through Sonogashira cross-coupling reaction in CH₃CN.

Cpd	X	R	Base	Ligand/Catalyst	Additive	Yield %
12a	O	Ph	Et ₃ N	Pd(PPh ₃) ₂ Cl ₂	CuI	75
12b	O	CH ₂ OCH ₂ Ph	Et ₃ N	Pd(PPh ₃) ₂ Cl ₂	CuI	38
12c	O	CH ₂ OH	K ₂ CO ₃	S-Phos/Pd(Oac) ₂	TBAI	75
13a	O	Ph	K ₂ CO ₃	S-Phos/Pd(Oac) ₂	TBAI	78
13b	O	(CH ₂) ₃ Ph	K ₂ CO ₃	S-Phos/Pd(Oac) ₂	TBAI	76
13c	O	CH ₂ OH	K ₂ CO ₃	S-Phos/Pd(Oac) ₂	TBAI	72
11	NCH ₃	Ph	K ₂ CO ₃	S-Phos/Pd(Oac) ₂	TBAI	78

Palladium-catalyzed Sonogashira cross-coupling is a widely used method to synthesize functional molecules containing an alkyne unit. Traditional Sonogashira coupling with Pd(PPh₃)₂Cl₂ (3.0 mol %) and Et₃N typically requires the use of a Cu(I) halide salt as a cocatalyst to have high reaction productivity. So, starting from coumarin **5b** and under these conditions, the phenyl acetylene moiety was introduced under microwave irradiation in 75% yield (cpd **12a**). However, with Obn propargylalcohol, the same conditions yielded **12b** in only 38% yield. Recently, Chorley et al. highlighted the efficacy of Pd(Oac)₂ and 2-dicyclohexylphosphino-2',6'-dimethoxybiphenyl (Sphos) as an effective catalytic system

for the Sonogashira cross-coupling reaction [46]. In addition, the presence of tetrabutylammonium iodide (TBAI) as an additive increased the yield of the reaction [47]. Under these conditions and without the protection of propargylic alcohol, we isolated the target alkyne derivative **12c** in 75% yield. These last conditions applied to Otf intermediates **4** and **5b** in the presence of various terminal alkynes, yielding target compounds **11** and **13a–c** in satisfactory yields (>70%, see Table 2) (Scheme 3).

Negishi cross-coupling reactions represent an extremely versatile tool for the introduction of alkyl substituents. As reported by Knochel et al. [48] and in the presence of Sphos (10.0 mol %) and Pd(OAc)₂ (5.0 mol %), it was possible to perform at room temperature an efficient cross-coupling reaction between Otf coumarin **5a–b** and benzyl zinc reagent (see Scheme 3, cpds **14** and **15**).

Lastly, the subsequent reduction of alkynes **12a** and **13a** was performed by catalytic hydrogenation, leading respectively to cpds **16** and **17**, as depicted in Scheme 3.

All synthesized compounds had their chemical structures confirmed by ¹H and ¹³C NMR and mass spectrometry, and all spectra data are available in the Supplementary Material.

2.2. Biological Evaluation

2.2.1. Effects of Coumarin Derivatives on Cell Viability

All the synthetic coumarins (**7**, **8a–f**, **9a–g**, **10**, **11**, **12a–c**, **13a–c**, **14–17**) were first screened for their *in vitro* cytotoxic activity at a single concentration (12 μM) against NSCLC cell line (human lung adenocarcinoma A549) for 24 h, using the well-established 3-(4,5-dimethylthiazol-2-yl)-2,5-diphenyltetrazolium bromide (MTT) assay. The results of A549 cells viability are reported in Figure 1.

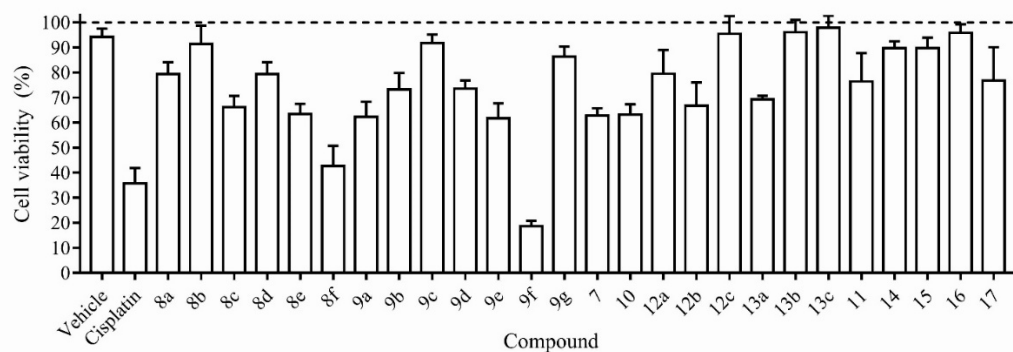


Figure 1. Effect of synthetic coumarin derivatives on cell viability. The viability of A549 cells was determined using the MTT assay after exposure at a single concentration (12 μM) of the compounds or cisplatin (2.6 μM) for 24 h. The percentage of inhibition was calculated considering the cells treated with medium (DMEM), which was considered as 100% of cell viability (dotted line). Bars represent the mean ± S.D. from three independent experiments.

The results showed that compounds **8b**, **9c**, **9g**, **12c**, **13b**, **13c**, **14**, **15**, and **16** showed little or no cytotoxicity. Compounds **7**, **8a**, **8c**, **8d**, **8e**, **9a**, **9b**, **9d**, **9e**, **10**, **11**, **12a–b**, **13a**, and **17** showed a moderate cytotoxicity by inducing a reduction in cell viability within 80–60%. Compounds **8f** and **9f**, which have in common the presence of a 3,4-dichloro-phenyl group ((3,4-Cl)-Ph), induced a strong cytotoxicity by decreasing the A549 cells viability to values below 50%.

Among these two compounds, **9f** was the most promising, reducing the A549 cells viability to less than 20%. Thus, this compound was selected and had its concentration that reduces the viable cell number by 50% (CC₅₀) determined against two cancer cell lines (human lung adenocarcinoma A549 and H2170 cell lines) and one non-cancer cell line (NIH-3T3), and showed CC₅₀ values (mean ± S.D.) of 7.1 ± 0.8 μM, 3.3 ± 0.5 μM, and 25.8 ± 1.7 μM against A549, H2170, and NHI-3T3 cells, respectively (Supplementary Materials II). Distinct explanations might be used to sustain this fact, including biochemical and metabolic changes between cell lines. While normal cells follow a set of organized

metabolic programs, cancer cells show intrinsic or acquired resistance to apoptosis and also a metabolic reprogramming in order to meet the increased energy demands [49]. Facing these results, we can note that **9f** showed to be the most potent against cancer cells (A549 and H2170 cell lines) than against healthy cell (NIH-3T3 cell line).

These cytotoxicity results are better than those observed for the most cytotoxic coumarins from other studies against the A549 cells, such as umbelliprenin ($IC_{50} = 52 \pm 1.97 \mu\text{M}$) [33]; 3-aryl coumarin derivative (8-(acetyloxy)-3-(4-methanesulfonyl phenyl)-2-oxo-2*H*-chromen-7-yl acetate) with $IC_{50} = 24.2 \mu\text{M}$ [31]; and iodinated-4-aryloxymethyl coumarins (6-chloro- and 7-chloro-4-(4-iodo-phenoxy methyl)-chromen-2-one) with $IC_{50} = 7.57 \mu\text{M}$ [35]; these latter bearing chlorine atoms in their structures, as observed in the most active compounds of the present study (coumarins **8f** and **9f**).

On the basis of cytotoxic effect, the concentration of $7 \mu\text{M}$ of **9f** was chosen for further to characterize the antitumor activity by investigating their effects on the process of inhibition of the EMT-associated migratory ability and epithelial-to-mesenchymal transition (EMT) in IL-1 β -stimulated A549 cells.

2.2.2. Effect of **9f** on IL-1 β -Induced EMT in A549 Cells

The EMT process is characterized by the phenotypic conversion of epithelial into mesenchymal cells that occurs with great frequency in fibrotic tissues, embryonic cells, and cancer. This transition increases the invasion capacity and the migratory potential of cells, which are characteristic of metastatic cancer, contributing additionally to the development of drug resistance in cancer [50–55].

To determine whether compound **9f** acts as an inhibitory compound of EMT in epithelial cells, the morphological changes induced by IL-1 β on A549 cells was observed. As shown in Figure 2A,B, the A549 cells maintained to culture medium (DMEM) or treated with compound **9f** exhibited, in a confluent monolayer, a cobblestone-like cell morphology, which is characteristic of epithelial cells. Cells treated with 1 ng/mL IL-1 β exhibited an evident morphological change and acquired a spindle-like morphology with the loss of cell–cell interactions that is a characteristic feature of mesenchymal cells (Figure 2C). A549 cells treated with **9f** exhibited an impairment in changes in its mesenchymal characteristics induced by IL-1 β (Figure 2D), suggesting that **9f** possesses inhibitory effects on IL-1 β -induced F-actin reorganization.

To evaluate the effect of compound **9f** on actin cytoskeleton organization, A549 cells were IL-1 β -stimulated and evaluated by staining with FITC-labeled phalloidin. As presented in Figure 2E,F, the A549 cells maintained to culture medium (DMEM) or treated with **9f** exhibited an abundant deposition of actin filament in the cortical region, which determines a cellular cobblestone-like morphology typical of epithelial cells. Stimulation with IL-1 β induced a cytoskeleton reorganization, leading to the activation of actin polymerization and the morphologic cell reorganization, which indicate a differentiation from the epithelial to mesenchymal phenotype (Figure 2G). Treatment with **9f** attenuated the changes in the actin cytoskeleton reorganization in A549 cells stimulated by IL-1 β (Figure 2H).

To corroborate whether this morphological transformation represents EMT, immunofluorescent staining was used to quantify the vimentin, which is a mesenchymal marker most commonly associated with EMT and involved in cancer progression [56].

As shown in Figure 3A,B, 24 h incubation with 1 ng/mL IL-1 β increased significantly the expression of vimentin in A549 cells compared with those maintained in DMEM medium (control). We found that the treatment of cells with **9f** ($7 \mu\text{M}$) significantly diminished the expression of mesenchymal marker vimentin in IL-1 β -stimulated A549 cells (Figure 3A,B), which is a phenomenon confirmed by the quantitative assessment by flow cytometry (Figure 3B–C). The treatment of cells with **9f** did not change the levels of vimentin expression in unstimulated cells with IL-1 β (Figure 3A–C). This result showed that **9f** treatment suppresses IL-1 β -induced EMT in A549 cells through downregulating vimentin.

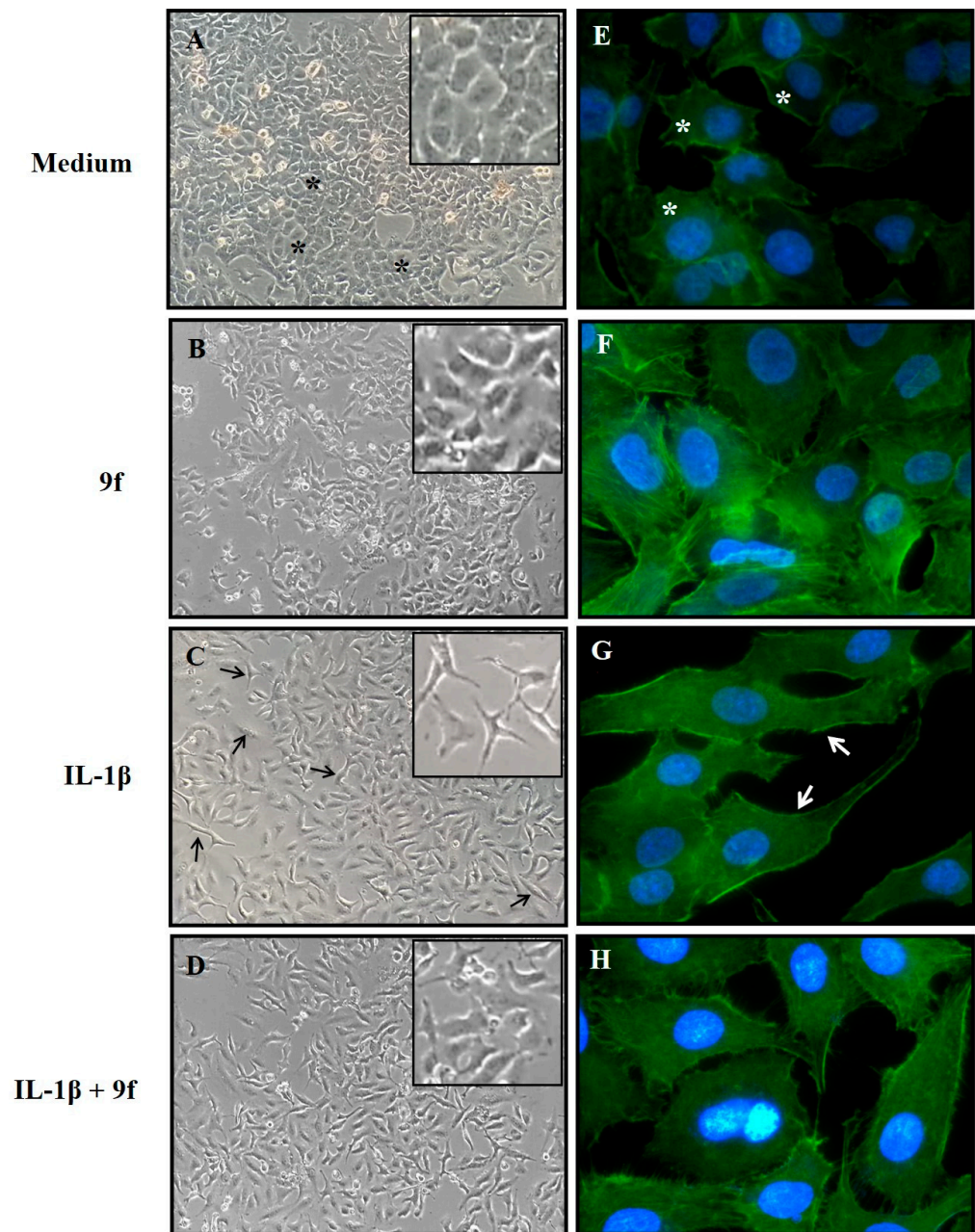


Figure 2. Compound **9f** inhibited IL-1 β -induced EMT in vitro. A549 cells were treated with **9f** (7 μ M) in the presence or absence of 1 ng/mL IL-1 β . Cells were photographed using phase-contrast microscopy (A–D) or fluorescence microscopy (E–H). Cells were exposure to treatment with DMEM-medium (A–E), **9f** (B–F), IL-1 β (C–G), or **9f** + IL-1 β (D–H) for 24 h. (Asterisks) Epithelial cells arranged in a cobblestone-like monolayer. (Arrowheads) Cells with an elongated, mesenchymal morphology. Actin (green) was detected via immunofluorescence in formaldehyde-fixed cells with FITC-conjugated phalloidin (1:100). Nuclei were counterstained with DAPI. Magnification $\times 100$ (insert, magnification $\times 200$) for phase-contrast microscope and $\times 400$ for fluorescence microscope.

Given the good results of **9f** in inhibiting the IL-1 β -induced EMT in epithelial cells, we investigated whether **9f** could affect the EMT-associated migratory ability in A549 cells. For this, in vitro wound-healing assay was performed to evaluate whether **9f** acts as an anti-metastatic agent in A549 cells.

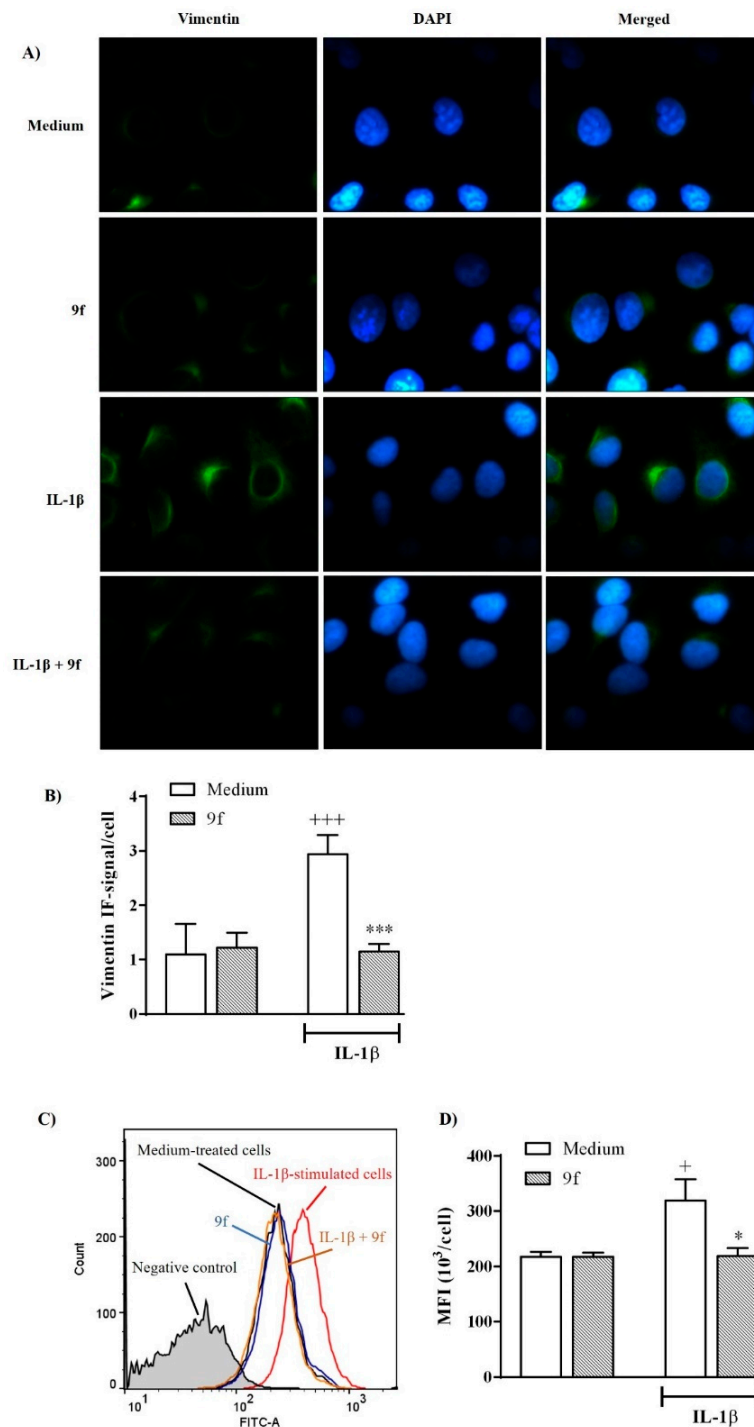


Figure 3. Compound **9f** downregulates the expression of mesenchymal cell marker vimentin in IL-1 β -induced EMT. A549 cells were treated with compound **9f** (7 μ M) in the presence or absence of 1 ng/mL IL-1 β . The mesenchymal markers vimentin was detected by immunofluorescence. (A) Cells were exposed to treatment with DMEM medium, **9f**, IL-1 β , or IL-1 β + **9f** for 24 h. Vimentin (green) was detected and measured (B) via immunofluorescence in formaldehyde-fixed cells with FITC-conjugated antibody. Nuclei were counterstained with DAPI. Magnification \times 400 for fluorescence microscope. (C,D) Flow cytometry analysis showing the reduced expression of vimentin in IL-1 β -induced EMT under **9f** treatment. In the graph in (C), bars represent the mean \pm S.D. from three independent experiments. (+) $p < 0.01$ and (+++) $p < 0.001$ compared with respective DMEM-treated cells and (*) $p < 0.01$ and (***) $p < 0.001$ compared with IL-1 β -stimulated cell medium-treated cells.

As shown in Figure 4A,B, IL-1 β -treated cells exhibited an increase in wound closure within 24 h compared with those not treated with IL-1 β (control). Treatment of cells with **9f** at 7 μ M for 24 h significantly reduced the migration of IL-1 β -stimulated cells, which is a phenomenon confirmed by qualitative assessment of the wound closure (Figure 4A,B).

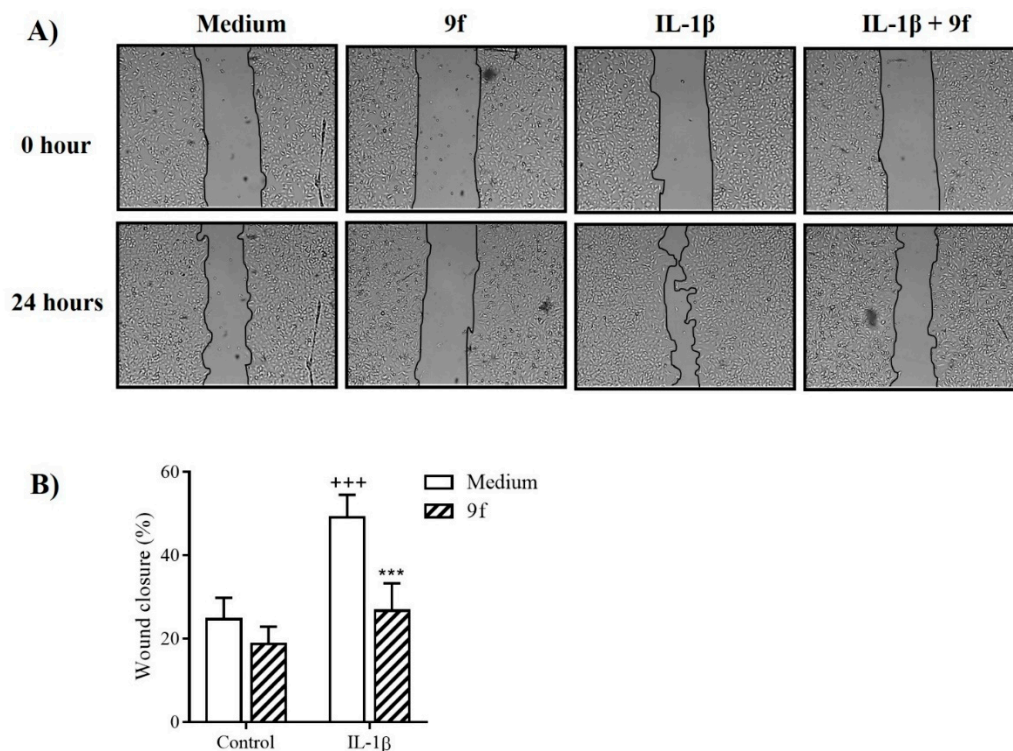


Figure 4. The effect of **9f** on the migration of A549 cells assayed by the wound-healing assay. Cells were treated with **9f** at 7 μ M, and images were captured to calculate the scratch closure. In (A), representative photomicrography images showing the cell migration toward the cell-free area after treatment with DMEM (control) or **9f** and after 24 h. In (B), the graph shows the percentage of scratch covered, which was measured by quantifying the total distance the cells moved from the edge of the scratch toward the center of the scratch, using ImageJ software, followed by conversion to a percentage of the wound covered. Values represent mean \pm S.D. from three independent experiments. (+++) $p < 0.001$ compared with respective DMEM-treated cells and (***) $p < 0.001$ compared with IL-1 β -stimulated cell vehicle-treated cells.

3. Materials and Methods

3.1. Compounds (Synthetic Coumarins)

Compounds **1d** [57], **3** [45], **5b** [58], **6** [59], **8a** [60], **8d** [46], **9a** [60], **9b** and **9c** [61], **9d** [59], **9g** [62], **10** [59], **12a** [63], **13a** [64], and **17** [65] were synthesized, and the structure of these compounds has been confirmed by comparison with NMR spectral data from the literature.

All other coumarin derivatives: triflic intermediates (**4**, **5a**, **5b**, **6**); Suzuki–Miyaura adducts (**7**, **8a–g**, **9a–f**); Sonogashira adducts **11**, **12a–c**, **13 a–c**); Negishi adducts (**14** and **15**); and alkyl coumarin derivatives obtained by catalytic hydrogenation (**16** and **17**) were prepared according to the synthetic procedures described in the Supplementary Material.

3.2. Biological Assays

3.2.1. Cell line and Cell Culture

A549, H2170, and normal mouse fibroblast (NIH-3T3) cell lines were obtained from the Rio de Janeiro Cell Bank (BCRJ). A549 and NIH-3T3 cells were maintained in Dulbecco's Modified Eagle Medium (DMEM), while the H2170 cell line was maintained in Roswell

Park Memorial Institute (RPMI)-1640. The culture media were supplemented with 10% fetal bovine serum (FBS), 2 mM L-glutamine, and 40 µg/mL gentamicin. All cells were cultured in a humidified atmosphere contained 5% CO₂ incubator at 37 °C. For experiments, cells were grown to 90% confluence. All experiments were conducted using cells with passage numbers less than 10.

3.2.2. Cell Viability Assay and Treatment

The effect of coumarin derivatives on cell viability was evaluated by the MTT assay at a single dose according to the NCI testing protocol or at different concentrations for IC₅₀ determination [66]. Coumarin derivatives were dissolved in dimethyl sulfoxide (DMSO) and then diluted with DMEM. Briefly, cells were plated in 96-well plates (2 × 10⁴/well) and each coumarin derivative at 12 µM was added to the culture medium, and the cell cultures were continued for 24 h. Cisplatin (2.6 µM) was used as a reference drug. Thereafter, the medium was replaced with fresh DMEM containing 5 mg/mL MTT. Following an incubation period (4 h) in a humidified CO₂ incubator at 37 °C and 5% CO₂, the supernatant was removed, and dimethyl sulfoxide solution (DMSO, 150 mL/well) was added to each cultured plate. After incubation at room temperature for 15 min, the absorbance of the solubilized MTT formazan product was spectrophotometrically measured at 540 nm. Three individual wells were assayed for each treatment, and the percentage viability relative to the control sample was determined as (absorbance of treated cells/absorbance of untreated cells) × 100%. Only the compound that reduced the viability by more than half the value of the control cells were screened in a range of concentration (10⁻⁸ to 10⁻³ M) with the A549, H2170, and NHI-3T3 cell lines. The concentration of **9f** compound that reduced the viable cell number by 50% (CC₅₀) was determined using a non-linear regression approach, and the mean value of CC₅₀ for each cell type was calculated from triplicate.

3.2.3. Epithelial-to-Mesenchymal Transition (EMT) Induction and Coumarin Derivatives Treatment

For induction of the EMT process, A549 cells (1 × 10⁵ per well) were seeded in 24-well culture plates and treated with 1 ng/mL IL-1β (Peprotech, Rocky Hill, NJ, USA) for 24 h. In the unstimulated cells, DMEM medium was added. Then, the morphological alteration of cells was observed under a microscope. This protocol for EMT induction is as reported in the previous literature [67]. To evaluate the effects of coumarin derivative with respect to EMT induced by IL-1β, cells were pretreated with compound **9f** at 7 µM, being this treatment also maintained during stimulation with IL-1β for 24 h.

3.2.4. Immunofluorescence Staining

After 24 h, cells were fixed for 15 min at 4 °C with 4% paraformaldehyde in PBS. Cells were permeabilized with 0.1% Triton X-100 and washed with PBS. Next, cells were incubated with FITC-conjugated phalloidin (1:100) for 2 h at room temperature and then rinsed several times with PBS. Following an additional washing step with PBS, cells were stained with 10 µg/mL DAPI at room temperature for 10 min for the visualization of cell nuclei. Cell morphology was determined using an inverted epifluorescence microscope (Nikon Eclipse 50i). Fluorescence quantification was done using ImageJ 1.47 software (NIH, Bethesda, MD, USA). Images were analyzed through the "Measure" menu, which allowed analyzing the fluorescence intensity signal per cell from original photomicrographs.

In another set of experiments, the analysis for vimentin, a well-recognized marker for its selective expression and specific role in the mesenchymal state, was performed. After treatment, cells were fixed, permeabilized, and washed as described above. Next, the slides were incubated with an anti-vimentin antibody (1:100) at 4 °C overnight. The next day, the slides were incubated with secondary antibody goat anti-rabbit-FITC (1:100) dilutions at room temperature for 1 h. Lastly, cells were stained with DAPI (Invitrogen; Thermo Fisher Scientific, Inc., Waltham, MA, USA) and washed with PBS. Stained cells were analyzed by a flow cytometer (FACSCanto II, Becton Dickinson, San Jose, CA, USA)

accompanied with the BD FACSDIVA™ software for data analysis. The cell-associated fluorescence of 5000 cells per sample was measured as mean fluorescence intensity (MFI) in the FL1 channel. The MFI values were corrected for unspecific staining by subtracting the fluorescence of cells unstained (negative control).

3.2.5. In Vitro Scratch Wound Healing Assay

To evaluate the effect of **9f** on epithelial motility, we performed the scratch assay as described by Cardoso et al. [68]. Cells were maintained in 24-well plates until they reached 90% confluency. Thereafter, a vertical stripe on the cell monolayer was made using a sterile pipette (200 µL) tip. The wells were washed with PBS to remove dead cells and debris, and then, **9f** was added at a concentration of 7 µM. As a control, the cells were treated with cell culture medium. Photographs were captured by a digital camera connected to an inverted microscope (Olympus IX70) at 0 and 24 h after scratch. The migration gap area of the cells was measured by ImageJ software (<https://imagej.nih.gov/ij/>; accessed on 24 November 2020, Center for Information Technology, National Institute of Health, Bethesda, MA, USA). Each measurement was repeated three times.

3.2.6. Statistical Analysis

Data were expressed as mean ± standard deviation (S.D.). The statistical analysis involving two groups was done using Student's *t*-test. Analysis of variance followed by the Tukey's test was used to compare three or more groups. Values of $p < 0.05$ were considered as indicative of significance.

4. Conclusions

In conclusion, twenty-six coumarin derivatives were synthesized through PCCCR and were evaluated for their anti-lung cancer properties against two non-small cell lung carcinoma (NSCLC) cell lines. Coumarins **8f** and **9f**, presenting a 3,4-dichloro-phenyl radical, inhibited in vitro the growth of both human lung adenocarcinoma cells in low micromolar concentration. Derivative **9f** regulates the epithelial-to-mesenchymal transition (EMT) suppressing the mesenchymal marker vimentin and cancer cell migration in IL-1β-stimulated A549 cells. Taken together, our findings suggest that coumarin derivatives, especially compound **9f**, may become a promising hit in the process of lung cancer drug discovery, especially in lung cancer promoted by non-small cell lung carcinoma (NSCLC) cell lines.

Supplementary Materials: The following supporting information can be downloaded at: <https://www.mdpi.com/article/10.3390/ph15010104/s1>, (I): All synthetic procedures and compounds characterization. All spectroscopy figures. (II): Cytotoxic concentration (CC50) of **9f** compound on A549, H2170 and NIH3T3 cells.

Author Contributions: Conceptualization, F.J.B.M.-J., E.B., J.-J.B. and M.S.; methodology, R.S.A.d.A., R.O.d.M., R.S.R., J.-J.B., M.S., N.B.d.M., J.d.O.d.S.C., S.L.d.O.S., C.R.A.C.d.S. and T.P.M.S.; validation, R.S.A.d.A., R.S.R., T.M.d.A., M.S. and J.d.O.d.S.C.; formal analysis, R.S.R., J.d.O.d.S.C. and T.P.M.S.; investigation, R.S.A.d.A., R.O.d.M., R.S.R., T.M.d.A., J.d.O.d.S.C., S.L.d.O.S., C.R.A.C.d.S. and T.P.M.S.; resources, F.J.B.M.-J., E.B., J.-J.B., M.S.; data curation, R.O.d.M., R.S.R., T.M.d.A., M.S.; writing—original draft preparation, R.S.A.d.A., E.B., T.M.d.A., N.B.d.M., J.d.O.d.S.C., S.L.d.O.S., C.R.A.C.d.S. and T.P.M.S.; writing—review and editing, R.S.A.d.A., F.J.B.M.-J., E.B., J.M.B.F., R.O.d.M., R.S.R., T.M.d.A., J.-J.B., M.S., J.d.O.d.S.C., S.L.d.O.S., C.R.A.C.d.S. and T.P.M.S.; supervision, F.J.B.M.-J., E.B., J.M.B.F., J.-J.B., M.S.; project administration, F.J.B.M.-J., E.B., T.M.d.A.; funding acquisition, F.J.B.M.-J., E.B., J.M.B.F., R.O.d.M., J.-J.B. All authors have read and agreed to the published version of the manuscript.

Funding: This research was funded by Conselho Nacional de Desenvolvimento Científico e Tecnológico (CNPq) [grant numbers 308590/2017-1 and 306798/2020-4]. This study was financed in part by the Coordenação de Aperfeiçoamento de Pessoal de Nível Superior—Brasil (CAPES)—Finance Code 001. We also thank Paraíba State Research Foundation (FAPESQ) grant number 301724/2021-0, and National Institute of Science and Technology in Neuroimmunomodulation (INCT-NIM/CNPq) for the scholarships provided to R.S.A.d.A. and J.d.O.d.S.C. respectively. The APC was funded by Universidade Estadual da Paraíba (UEPB) [grant 001/2021].

Institutional Review Board Statement: Not applicable.

Informed Consent Statement: Not applicable.

Data Availability Statement: The data presented in this study are available in article and Supplementary Material.

Acknowledgments: This work was supported by the Federal University of Alagoas (UFAL) and State University of Paraíba (UEPB).

Conflicts of Interest: The authors declare no conflict of interest. The funders had no role in the design of the study; in the collection, analyses, or interpretation of data; in the writing of the manuscript, or in the decision to publish the results.

References

1. Zafar, S.N.; Siddiqui, A.H.; Channa, R.; Ahmed, S.; Javed, A.A.; Bafford, A. Estimating the Global Demand and Delivery of Cancer Surgery. *World J. Surg.* **2019**, *43*, 2203–2210. [\[CrossRef\]](#)
2. Bray, F.; Ferlay, J.; Soerjomataram, I.; Siegel, R.L.; Torre, L.A.; Jemal, A. Global cancer statistics 2018: GLOBOCAN estimates of incidence and mortality worldwide for 36 cancers in 185 countries. *CA Cancer J. Clin.* **2018**, *68*, 394–424. [\[CrossRef\]](#)
3. Ganesh, K.; Massagué, J. Targeting metastatic cancer. *Nat. Med.* **2021**, *27*, 24–44. [\[CrossRef\]](#)
4. Lambert, A.W.; Pattabiraman, D.R.; Weinberg, R.A. Emerging Biological Principles of Metastasis. *Cell* **2017**, *168*, 670–691. [\[CrossRef\]](#)
5. Lamouille, S.; Xu, J.; Derynck, R. Molecular mechanisms of epithelial-mesenchymal transition. *Nat. Rev. Mol. Cell Biol.* **2014**, *15*, 178–196. [\[CrossRef\]](#)
6. Lu, W.; Kang, Y. Epithelial-Mesenchymal Plasticity in Cancer Progression and Metastasis. *Dev. Cell* **2019**, *49*, 361–374. [\[CrossRef\]](#)
7. Dongre, A.; Weinberg, R.A. New insights into the mechanisms of epithelial-mesenchymal transition and implications for cancer. *Nat. Rev. Mol. Cell Biol.* **2019**, *20*, 69–84. [\[CrossRef\]](#)
8. Pearson, G.W. Control of Invasion by Epithelial-to-Mesenchymal Transition Programs during Metastasis. *J. Clin. Med.* **2019**, *8*, 646. [\[CrossRef\]](#)
9. Marcucci, F.; Stassi, G.; De Maria, R. Epithelial-mesenchymal transition: A new target in anticancer drug discovery. *Nat. Rev. Drug Discov.* **2016**, *15*, 311–325. [\[CrossRef\]](#)
10. Cho, E.S.; Kang, H.E.; Kim, N.H.; Yook, J.I. Therapeutic implications of cancer epithelial-mesenchymal transition (EMT). *Arch. Pharm. Res.* **2019**, *42*, 14–24. [\[CrossRef\]](#)
11. Araújo, R.S.A.; Mendonça, F.J.B., Jr. Coumarins: Synthetic Approaches and Pharmacological Importance. In *Natural Products and Drug Discovery: From Pharmacology to Pharmacological Approaches*, 1st ed.; Diniz, M.F.F.M., Scotti, L., Scotti, M.T., Alves, M.F., Eds.; Editora UFPB: João Pessoa, Brazil, 2018; pp. 245–274.
12. Zhang, S.-G.; Liang, C.-G.; Sun, Y.-Q.; Teng, P.; Wang, J.-Q.; Zhang, W.-H. Design, synthesis and antifungal activities of novel pyrrole- and pyrazole-substituted coumarin derivatives. *Mol. Divers.* **2019**, *23*, 915–925. [\[CrossRef\]](#)
13. Mahmoodi, N.O.; Jalalifard, Z.; Fathanbari, G.P. Green synthesis of bis-coumarin derivatives using Fe(III) as a catalyst and investigation of their biological activities. *J. Chin. Chem. Soc.* **2020**, *67*, 172–182. [\[CrossRef\]](#)
14. Al-Majedy, Y.K.; Ibraheem, H.H.; Jassim, L.S.; Al-Amiry, A.A. Antioxidant activity of coumarin compounds. *ANJS* **2019**, *22*, 1–8. [\[CrossRef\]](#)
15. Wang, T.; Peng, T.; Wen, X.; Wang, G.; Liu, S.; Sun, Y.; Zhang, S.; Wang, L. Design, synthesis and evaluation of 3-substituted coumarin derivatives as anti-inflammatory agents. *Chem. Pharm. Bull.* **2020**, c19-01085. [\[CrossRef\]](#)
16. Mohamed, T.K.; Batran, R.Z.; Elseginy, S.A.; Ali, M.M.; Mahmoud, A.E. Synthesis, anticancer effect and molecular modeling of new thiazolopyrazolyl coumarin derivatives targeting VEGFR-2 kinase and inducing cell cycle arrest and apoptosis. *Bioorg. Chem.* **2019**, *85*, 253–273. [\[CrossRef\]](#)
17. Kasperkiewicz, K.; Ponczek, M.B.; Owczarek, J.; Guga, P.; Budzisz, E. Antagonists of vitamin K—Popular coumarin drugs and new synthetic and natural coumarin derivatives. *Molecules* **2020**, *25*, 1465. [\[CrossRef\]](#)
18. Thornes, R.D.; Daly, L.; Lynch, G.; Breslin, B.; Browne, H.; Browne, H.Y.; Corrigan, T.; Daly, P.; Edwards, G.; Gaffney, E.; et al. Treatment with coumarin to prevent or delay recurrence of malignant melanoma. *J. Cancer Res. Clin. Oncol.* **1994**, *120*, S32–S34. [\[CrossRef\]](#)
19. Marshall, M.E.; Mohler, J.L.; Edmonds, K.; Williams, B.; Butler, K.; Ryles, M.; Weiss, L.; Urban, D.; Bueschen, A.; Markiewicz, M.; et al. An updated review of the clinical development of coumarin (1,2-benzopyrone) and 7-hydroxycoumarin. *J. Cancer Res. Clin. Oncol.* **1994**, *120*, S39–S42. [\[CrossRef\]](#)

20. von Angerer, E.; Kager, M.; Maucher, A. Anti-tumour activity of coumarin in prostate and mammary cancer models. *J. Cancer Res. Clin. Oncol.* **1994**, *120*, S14–S16. [[CrossRef](#)]
21. Lopez-Gonzalez, J.S.; Prado-Garcia, H.; Aguilar-Cazares, D.; Molina-Guarneros, J.A.; Morales-Fuentes, J.; Mandoki, J.J. Apoptosis and cell cycle disturbances induced by coumarin and 7-hydroxycoumarin on human lung carcinoma cell lines. *Lung Cancer.* **2004**, *43*, 275–283. [[CrossRef](#)]
22. Emami, S.; Dadashpour, S. Current developments of coumarin-based anti-cancer agents in medicinal chemistry. *Eur. J. Med. Chem.* **2015**, *102*, 611–630. [[CrossRef](#)]
23. Dandriyal, J.; Singla, R.; Kumar, M.; Jaitak, V. Recent developments of C-4 substituted coumarin derivatives as anticancer agents. *Eur. J. Med. Chem.* **2016**, *119*, 141–168. [[CrossRef](#)]
24. Thakur, A.; Singla, R.; Jaitak, V. Coumarins as anticancer agents: A review on synthetic strategies, mechanism of action and SAR studies. *Eur. J. Med. Chem.* **2015**, *101*, 476–495. [[CrossRef](#)] [[PubMed](#)]
25. Zhang, L.; Xu, Z. Coumarin-containing hybrids and their anticancer activities. *Eur. J. Med. Chem.* **2019**, *181*, 111587. [[CrossRef](#)]
26. Klenkar, J.; Molnar, M. Natural and synthetic coumarins as potential anticancer agents. *J. Chem. Pharm. Res.* **2015**, *7*, 1223–1238.
27. Kawaii, S.; Tomono, Y.; Ogawa, K.; Sugiura, M.; Yano, M.; Yoshizawa, Y. The anti-proliferative effect of coumarins on several cancer cell lines. *Anticancer Res.* **2001**, *21*, 917–923.
28. Kumar, M.; Singla, R.; Dandriyal, J.; Jaitak, V. Coumarin Derivatives as Anticancer Agents for Lung Cancer Therapy: A Review. *Anti-Cancer Agents Med. Chem.* **2018**, *8*, 964–984. [[CrossRef](#)] [[PubMed](#)]
29. Weng, K.G.; Yuan, Y.L. Synthesis and evaluation of coumarin derivatives against human lung cancer cell lines. *Braz. J. Med. Biol. Res.* **2017**, *50*, e6455. [[CrossRef](#)] [[PubMed](#)]
30. Wang, Y.; Li, C.F.; Pan, L.M.; Gao, Z.L. 7,8-Dihydroxycoumarin inhibits A549 human lung adenocarcinoma cell proliferation by inducing apoptosis via suppression of Akt/NF- κ B signaling. *Exp. Ther. Med.* **2013**, *5*, 1770–1774. [[CrossRef](#)] [[PubMed](#)]
31. Musa, M.A.; Joseph, M.Y.; Latinwo, L.M.; Badisa, V.; Cooperwood, J.S. In vitro evaluation of 3-arylcoumarin derivatives in A549 cell line. *Anticancer Res.* **2015**, *35*, 653–659. [[PubMed](#)]
32. Musa, M.A.; Badisa, L.D.V.; Latinwo, L.M.; Patterson, T.A.; Owens, A.M. Coumarin-based Benzopyranone Derivatives Induced Apoptosis in Human Lung (A549) Cancer Cells. *Anticancer Res.* **2012**, *32*, 4271–4276.
33. Khaghanzadeh, N.; Mojtahedi, Z.; Ramezani, M.; Erfani, N.; Ghaderi, A. Umbelliprenin is cytotoxic against QU-DB large cell lung cancer cell line but anti-proliferative against A549 adenocarcinoma cells. *DARU J. Pharm. Sci.* **2012**, *20*, 69–74. [[CrossRef](#)]
34. Xiaoman, X.; Zhang, Y.; Qu, D.; Jiang, T.; Li, S. Osthole induces G2/M arrest and apoptosis in lung cancer A549 cells by modulating PI3K/Akt pathway. *J. Exp. Clin. Cancer Res.* **2011**, *30*, 33.
35. Basanagouda, M.; Jambagi, V.B.; Barigidad, N.N.; Laxmeshwar, S.S.; Devaru, V. Narayanachar. Synthesis, structure-activity relationship of iodinated-4-aryloxymethyl-coumarins as potential anti-cancer and anti-mycobacterial agents. *Eur. J. Med. Chem.* **2014**, *74*, 225–233. [[CrossRef](#)]
36. Belluti, F.; Fontana, G.; Dal Bo, L.; Carenini, N.; Giommarelli, C.; Zunino, F. Design, synthesis and anticancer activities of stilbene-coumarin hybrid compounds: Identification of novel proapoptotic agents. *Bioorg. Med. Chem.* **2010**, *18*, 3543–3550. [[CrossRef](#)]
37. Chen, Y.; Liu, H.R.; Liu, H.S.; Cheng, M.; Xia, P.; Qian, K.; Wu, P.C.; Lai, C.Y.; Xia, Y.; Yang, Z.Y.; et al. Antitumor agents 292. Design, synthesis and pharmacological study of S- and O-substituted 7-mercapto- or hydroxy-coumarins and chromones as potent cytotoxic agents. *Eur. J. Med. Chem.* **2012**, *49*, 74–85. [[CrossRef](#)]
38. Borges, F.; Roleira, F.; Milhazes, N.; Santana, L.; Uriarte, E. Simple coumarins and analogues in medicinal chemistry: Occurrence, synthesis and biological activity. *Curr. Med. Chem.* **2005**, *12*, 887–916. [[CrossRef](#)] [[PubMed](#)]
39. Lake, B.G. Coumarin metabolism, toxicity and carcinogenicity: Relevance for human risk assessment. *Food Chem. Toxicol.* **1999**, *37*, 423–453. [[CrossRef](#)]
40. Littke, A.F.; Fu, G.C. Palladium-catalyzed coupling reactions of aryl chlorides. *Angew. Chem. Int. Ed. Engl.* **2002**, *41*, 4176–4211. [[CrossRef](#)]
41. Mori, A.; Ahmed, M.S.M.; Sekiguchi, A.; Masui, K.; Koike, T. Sonogashira coupling with aqueous ammonia. *Chem. Lett.* **2002**, *31*, 756–757. [[CrossRef](#)]
42. Bellina, F.; Carpita, A.; Rossi, R. Palladium catalysts for the Suzuki cross-coupling reaction: An overview of recent advances. *Synthesis* **2004**, *2004*, 2419–2440. [[CrossRef](#)]
43. Tang, Z.-Y.; Hu, Q.-S. Room temperature nickel(0)-catalyzed suzuki-miyaura cross-couplings of activated alkenyl tosylates: Efficient synthesis of 4-substituted coumarins and 4-substituted 2-(5H)-furanones. *Adv. Synth. Catal.* **2004**, *346*, 1635–1637. [[CrossRef](#)]
44. Završnik, D.; Muratović, S.; Makuc, D.; Plavec, J.; Cetina, M.; Nagl, A.; De Clercq, E.; Balzarini, J.; Mintas, M. Benzylidene-bis-(4-hydroxycoumarin) and benzopyrano-coumarin derivatives: Synthesis, $^1\text{H}/^{13}\text{C}$ -NMR conformational and X-ray crystal structure studies and in vitro antiviral activity evaluations. *Molecules* **2011**, *16*, 6023–6040. [[CrossRef](#)] [[PubMed](#)]
45. Spadafora, M.; Postupalenko, V.Y.; Shvadchak, V.V.; Klymchenko, A.S.; Mély, Y.; Burger, A.; Benhida, R. Efficient synthesis of ratiometric fluorescent nucleosides featuring 3-hydroxychromone nucleobases. *Tetrahedron* **2009**, *65*, 7809–7816. [[CrossRef](#)]
46. Yamaguchi, Y.; Nishizono, N.; Kobayashi, D.; Yoshimura, T.; Wada, K.; Oda, K. Evaluation of synthesized coumarin derivatives on aromatase inhibitory activity. *Bioorg. Med. Chem. Lett.* **2017**, *27*, 2645–2649. [[CrossRef](#)] [[PubMed](#)]
47. Chorley, D.F.; Furkert, D.P.; Brimble, M.A. Synthesis of the spiroketal core of the pinnatifinoside family of natural products. *Eur. J. Org. Chem.* **2016**, *2016*, 314–319. [[CrossRef](#)]

48. Manolikakes, G.; Dong, Z.; Mayr, H.; Li, J.; Knochel, P. Negishi Cross-Coupling Compatible with Unprotected Amide Functions. *Chem. Eur. J.* **2009**, *15*, 1324–1328. [[CrossRef](#)]
49. Kalyanaraman, B. Teaching the basics of cancer metabolism: Developing antitumor strategies by exploiting the differences between normal and cancer cell metabolism. *Redox Biol.* **2017**, *12*, 833–842. [[CrossRef](#)]
50. Gavert, N.; Ben-Ze'ev, A. Epithelial-mesenchymal transition and the invasive potential of tumors. *Trends Mol. Med.* **2008**, *14*, 199–209. [[CrossRef](#)]
51. Bruzzese, F.; Leone, A.; Rocco, M.; Carbone, C.; Piro, G.; Caraglia, M.; Di Gennaro, E.; Budillon, A. HDAC inhibitor vorinostat enhances the antitumor effect of gefitinib in squamous cell carcinoma of head and neck by modulating ErbB receptor expression and reverting EMT. *J. Cell Physiol.* **2011**, *226*, 2378–2390. [[CrossRef](#)]
52. Valastyan, S.; Weinberg, R.A. Tumor metastasis: Molecular insights and evolving paradigms. *Cell* **2011**, *147*, 275–292. [[CrossRef](#)] [[PubMed](#)]
53. Arias, A.M. Epithelial mesenchymal interactions in cancer and development. *Cell* **2001**, *105*, 425–431. [[CrossRef](#)]
54. Kalluri, R.; Weinberg, R.A. The basics of epithelial-mesenchymal transition. *J. Clin. Investig.* **2009**, *119*, 1420–1428. [[CrossRef](#)]
55. Yan, L.; Yu, H.H.; Liu, Y.S.; Wang, Y.S.; Zhao, W.H. Esculetin enhances the inhibitory effect of 5-Fluorouracil on the proliferation, migration and epithelial-mesenchymal transition of colorectal cancer. *Cancer Biomark.* **2019**, *24*, 231–240. [[CrossRef](#)] [[PubMed](#)]
56. Jiang, Y.N.; Ni, X.Y.; Yan, H.Q.; Shi, L.; Lu, N.N.; Wang, Y.N.; Li, Q.; Gao, F.G. Interleukin 6-triggered ataxia-telangiectasia mutated kinase activation facilitates epithelial-to-mesenchymal transition in lung cancer by upregulating vimentin expression. *Exp. Cell Res.* **2019**, *381*, 165–171. [[CrossRef](#)]
57. Wang, T.-C.; Chen, Y.-L.; Tzeng, C.-C.; Liou, S.-S.; Tzeng, W.-F.; Chang, Y.-L.; Teng, C.-M. α -Methylidene- γ -butyrolactones: Synthesis and evaluation of quinolin-2(1H)-one derivatives. *Helv. Chim. Acta* **1998**, *81*, 1038–1047. [[CrossRef](#)]
58. Plougastel, L.; Pattanayak, M.R.; Riomet, M.; Bregant, S.; Sallustrau, A.; Nothisen, M.; Wagner, A.; Audisio, D.; Taran, F. Sydnone-based turn-on fluorogenic probes for no-wash protein labeling and in-cell imaging. *Chem. Commun.* **2019**, *55*, 4582–4585. [[CrossRef](#)]
59. Kumar, A.; Rao, M.L.N. Pot-economic synthesis of diarylpyrazoles and pyrimidines involving Pd-catalyzed cross-coupling of 3-trifloxochromone and triarylbiometh. *J. Chem. Sci.* **2018**, *130*, 165–175. [[CrossRef](#)]
60. Starčević, Š.; Brožič, P.; Turk, S.; Cesar, J.; Rižner, T.L.; Gobec, S. Synthesis and biological evaluation of (6- and 7-phenyl) coumarin derivatives as selective nonsteroidal inhibitors of 17 β -hydroxysteroid dehydrogenase type 1. *J. Med. Chem.* **2011**, *54*, 248–261. [[CrossRef](#)]
61. Das, S.G.; Srinivasan, B.; Hermanson, D.L.; Bleeker, N.P.; Doshi, J.M.; Tang, R.; Beck, W.T.; Xing, C. Structure-activity relationship and molecular mechanisms of ethyl 2-amino-6-(3,5-dimethoxyphenyl)-4-(2-ethoxy-2-oxoethyl)-4H-chromene-3-carboxylate (CXL017) and its analogues. *J. Med. Chem.* **2011**, *54*, 5937–5948. [[CrossRef](#)]
62. Aridoss, G.; Zhou, B.; Hermanson, D.L.; Bleeker, N.P.; Xing, C. Structure-activity relationship (SAR) study of ethyl 2-amino-6-(3,5-dimethoxyphenyl)-4-(2-ethoxy-2-oxoethyl)-4H-chromene-3-carboxylate (CXL017) and the potential of the lead against multidrug resistance in cancer treatment. *J. Med. Chem.* **2012**, *55*, 5566–5581. [[CrossRef](#)]
63. Peng, L.; Jiang, J.; Peng, C.; Dai, N.; Tang, Z.; Jiao, Y.; Chen, J.; Xu, X. Synthesis of Unsymmetrical Aromatic Acetylenes by Diphenyl Chlorophosphate-Promoted Condensation Reaction of Aromatic Aldehydes and Sulfones. *Chin. J. Org. Chem.* **2017**, *37*, 3013–3018. [[CrossRef](#)]
64. Elangovan, A.; Lin, J.-H.; Yang, S.-W.; Hsu, H.-Y.; Ho, T.-I. Synthesis and electrogenerated chemiluminescence of donor-substituted phenylethylcoumarins. *J. Org. Chem.* **2004**, *69*, 8086–8092. [[CrossRef](#)] [[PubMed](#)]
65. Yadav, C.; Maka, V.K.; Payra, S.; Moorthy, J.N. Multifunctional porous organic polymers (POPs): Inverse adsorption of hydrogen over nitrogen, stabilization of Pd(0) nanoparticles, and catalytic cross-coupling reactions and reductions. *J. Catal.* **2020**, *284*, 61–71. [[CrossRef](#)]
66. Geran, R.I.; Greenberg, N.H.; MacDonald, M.M.; Schumacher, A.; Abbott, B.J. Protocols for screening chemical agents and natural products against animal tumors and other biological systems. *Cancer Chemoth. Rep.* **1972**, *3*, 17–27.
67. Wang, J.; Bao, L.; Yu, B.; Liu, Z.; Han, W.; Deng, C.; Guo, C. Interleukin-1 β Promotes Epithelial-Derived Alveolar Elastogenesis via α v β 6 Integrin-Dependent TGF- β Activation. *Cell Physiol. Biochem.* **2015**, *36*, 2198–2216. [[CrossRef](#)]
68. Cardoso, S.H.; de Oliveira, C.R.; Guimarães, A.S.; Nascimento, J.; de Oliveira Dos Santos Carmo, J.; de Souza Ferro, J.N.; de Carvalho Correia, A.C.; Barreto, E. Synthesis of newly functionalized 1,4-naphthoquinone derivatives and their effects on wound healing in alloxan-induced diabetic mice. *Chem. Biol. Interact.* **2018**, *291*, 55–64. [[CrossRef](#)]